



Study of Thermal Behavior of Wall of a Cylindrical Calorimetric Vase Covered with Flax

Djibril NDIAYE¹, Lemrabott ould Habiboulah ¹, Issa DIAGNE¹, Youssou TRAORE¹, Seydou FAYE¹, Baba MBENGUE², Gregoire SISSOKO¹

¹Laboratory of Semiconductors and Solar Energy, Physics Department, Faculty of Science and Technology, University Cheikh Anta Diop, Dakar, Senegal

²Univerty of Thiès, Thiès, Senegal

Abstract Use of flax as thermal insulation on a cylindrical calorimeter is proposed in this study. Flax used has medium diffusivity $\alpha = 8.10^{-7} \text{ m}^2.\text{s}^{-1}$ and average thermal conductivity $\lambda = 0,037 \text{ W.m}^{-1}.\text{K}^{-1}$. Thermal behavior of flax material is highlighted from the study of temperature and heat flow density curves.

Spectroscopic study from Bode diagrams and Nyquist representation of thermal impedance and its phase showed the quality of thermal insulation. Thermoelectric parameters such as series resistance and shunt resistor have made it possible to characterize the material.

Keywords Flax-Temperature - Series resistance - Shunt resistance

1. Introduction

Artificial or synthetic insulation [1, 2] is a threat to the environment unlike natural insulation that is biodegradable and renewable. Studies on heat transfer have shown that these natural insulators (tow, kapok, sawdust ...) have a very good thermal insulation property [3, 4]. Studies on different models [5, 6, 7] have shown the quality of some thermal insulators such as tow or kapok.

In this study, we characterize the thermal behavior of flax over a hollow aluminum cylinder filled with a warm homogeneous liquid solution. We follow the thermal inertia of the filasse material from the study of the evolution curves of the temperature and the density of heat flow in dynamic frequency regime.

Calorimetric times or periods of measurement are relatively short which corresponds to relatively high excitatory pulsations (high frequencies). We thus analyze the Bode diagrams and the Nyquist representations by showing the behavior of the high-frequency material.

2. Theory

2.1. Scheme of study device

Different outer surfaces of calorimeter are considered subject to same external climatic constraints. Calorimeter is considered a closed system. Initial temperature of the fluid in calorimetric vessel is everywhere same.

2.2. Mathematical model

We consider that system is in cylindrical symmetry. Equation of heat (1) is obtained by considering that material does not contain an internal source of heat.

$$\frac{\partial^2 T}{\partial r^2} + \frac{1}{r} \frac{\partial T}{\partial r} + \frac{\partial^2 T}{\partial z^2} - \frac{1}{\alpha} \frac{\partial T}{\partial t} = 0 \quad (1)$$

$$\alpha = \frac{\lambda}{\rho.C} \quad (2)$$



λ = thermal conductivity
 ρ = density of the material
 C= massic heat

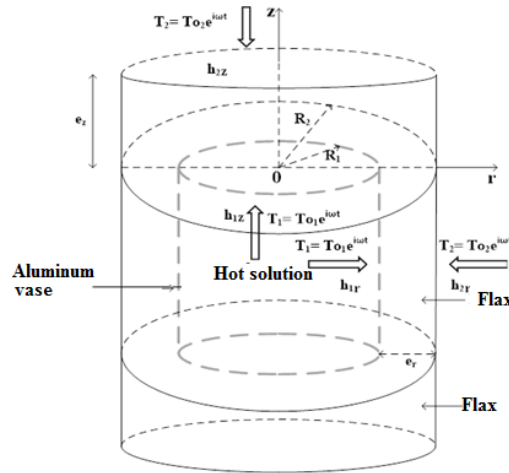


Figure 1: Schematic of calorimeter

T_1 : Temperature inside solution.	$T_1 = T_{01}e^{i\omega t}$ with $T_{01} = 90^{\circ}\text{C}$
T_2 : Ambient temperature	$T_2 = T_{02}e^{i\omega t}$ with $T_{02} = 27^{\circ}\text{C}$
T_i : Initial temperature of flax	$T_i = 25^{\circ}\text{C}$
R_1 : Inner radius of flax layer	$R_1 = 0.05 \text{ m}$
R_2 : outer radius of flax layer	$R_2 = 0.065 \text{ m}$
$e_r = R_2 - R_1$: thickness of insulation in radial direction	$e_r = e_z = e = 0.015 \text{ m}$
e_z : thickness of insulation along z axis	

Solution of equation (1) in dynamic frequency regime is given by equation (3):

$$T(r, z, \omega, t) = \sum_{j=1}^{\infty} [A_j \sinh(\beta_j z) + B_j \cosh(\beta_j z)] J_0(\mu_j r) e^{i\omega t} + T_i \tag{3}$$

With

$$J_0(\mu_j r) = \sum_{m=1}^{\infty} \frac{(-1)^m (\mu_j r)^{2m}}{4^m m! m!} \tag{4}$$

We obtain expressions of components A_j and B_j from equations (5) and (6). Equations (7) and (8) make it possible to obtain eigenvalues which are determined graphically from transcendental equations (9) and (11).

$$\lambda \frac{\partial T}{\partial z} \Big|_{z=0} = h_{1z} [T(r, 0, \omega, t) - T_1] \tag{5}$$

$$-\lambda \frac{\partial T}{\partial z} \Big|_{z=e} = h_{2z} [T(r, e, \omega, t) - T_1] \tag{6}$$

$$-\lambda \frac{\partial T}{\partial r} \Big|_{r=R_1} = h_{1r} [T_1 - T(R_1, z, \omega, t)] \tag{7}$$

$$\lambda \frac{\partial T}{\partial r} \Big|_{r=R_2} = h_{2r} [T_2 - T(R_2, z, \omega, t)] \tag{8}$$

$$\frac{\lambda \mu_j}{h_{1r} h_{2r}} = \frac{J_0(\mu_j R_2) [-T_{01} + T_i e^{-i\omega t}] + J_0(\mu_j R_1) [T_{02} - T_i e^{-i\omega t}]}{h_{1r} J_1(\mu_j R_2) [-T_{01} + T_i e^{-i\omega t}] + h_{2r} J_1(\mu_j R_1) [-T_{02} + T_i e^{-i\omega t}]} \tag{9}$$

we pose :

$$n_j = e \cdot \mu_j \tag{10}$$

$$g(n_j) = \frac{\lambda n_j}{h_{1r} h_{2r} e} \text{ and } f(n_j) = \frac{J_0(\frac{n_j R_2}{e}) [-T_{01} + T_i e^{-i\omega t}] + J_0(\frac{n_j R_1}{e}) [T_{02} - T_i e^{-i\omega t}]}{h_{1r} J_1(\frac{n_j R_2}{e}) [-T_{01} + T_i e^{-i\omega t}] + h_{2r} J_1(\frac{n_j R_1}{e}) [-T_{02} + T_i e^{-i\omega t}]} \tag{11}$$

We graphically determine the eigenvalues n_j and μ_j .

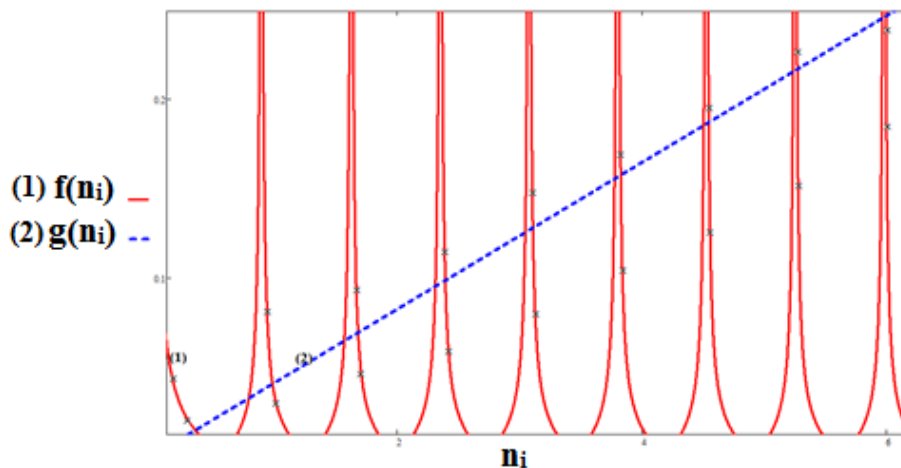


Figure 2: Graphical determination of eigenvalues μ_j
 $h_{1r} = 60 \text{ (W/m}^2\text{.K)}$; $h_{2r} = 1 \text{ (W/m}^2\text{.K)}$ $\omega = 0.001 \text{ rad.s}^{-1}$.

Table 1: Eigenvalues

n_j	0.35	0.978	1.677	2.39	3.106	3.825	4.546	5.268
μ_j	23.333	65.2	111.8	159.333	207.067	255	303.067	351.2

Expression (12) gives the density of heat flow through flax material.

$$\phi(r, z, \omega, t) = \left\{ \lambda^2 \sum_{j=1}^{\infty} \left[e^{i\omega t} \cdot \mu_j \cdot J_1(\mu_j \cdot r) \cdot (A_j \sinh(\beta_j \cdot z) + B_j \cdot \cosh(\beta_j \cdot z)) \right]^2 + \lambda^2 \sum_{j=1}^{\infty} \left[e^{i\omega t} \cdot J_0(\mu_j \cdot r) \cdot (A_j \cdot \beta_j \cosh(\beta_j \cdot z) + B_j \cdot \beta_j \sinh(\beta_j \cdot z)) \right]^2 \right\}^{\frac{1}{2}} \tag{12}$$

By analogy with Ohm's law, we write:
 $\Delta T(r, z, \omega, t) = T(r, 0, \omega, t) - T(r, z, \omega, t) = Z_{th}(r, z, \omega, t) \cdot \phi(r, z, \omega, t)$ (13)

Relation (14) expresses temperature variation inside material.

$$T(r, 0, \omega, t) - T(r, z, \omega, t) = \sum_{j=1}^{\infty} [B_j (1 - \cosh(\beta_j \cdot z)) - A_j \cdot \sinh(\beta_j \cdot z)] J_0(\mu_j \cdot r) \cdot e^{i\omega t} \tag{14}$$

Taking into account expression (13), expression (15) of thermal impedance of flax is obtained.

$$Z_{th}(r, z, \omega, t) = \frac{\sum_{j=1}^{\infty} [B_j(1 - \cosh(\beta_j \cdot z)) - A_j \cdot \sinh(\beta_j \cdot z)] J_0(\mu_j \cdot r) \cdot e^{i\omega t}}{\phi(r, z, \omega, t)} \tag{15}$$

3. Results

3.1. Evolution of temperature and density of heat flux in flax

Figures (3) and (4) respectively show changes in temperature and heat flow density on the base (or lid) of the calorimeter. Figures (5) and (6) show changes in temperature and heat flow density on side wall of the calorimeter. In these different evolutions, we highlight influence of excitatory pulsation.

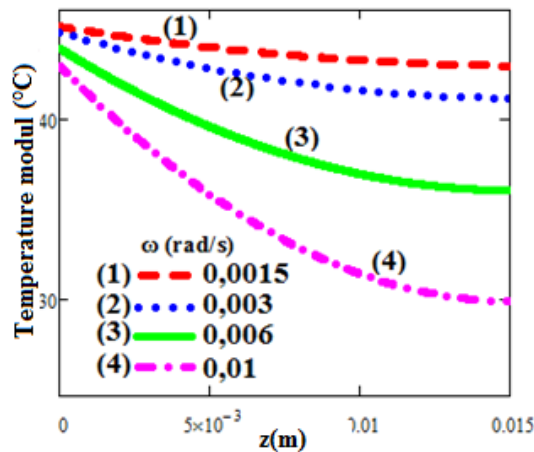


Figure 3: Evolution of temperature on cover of calorimeter.

$r = 0.055 \text{ m}$; $h_{1z} = 25 \text{ W}/(\text{m}^2 \cdot \text{K})$; $h_{2z} = 0.05 \text{ W}/(\text{m}^2 \cdot \text{K})$.

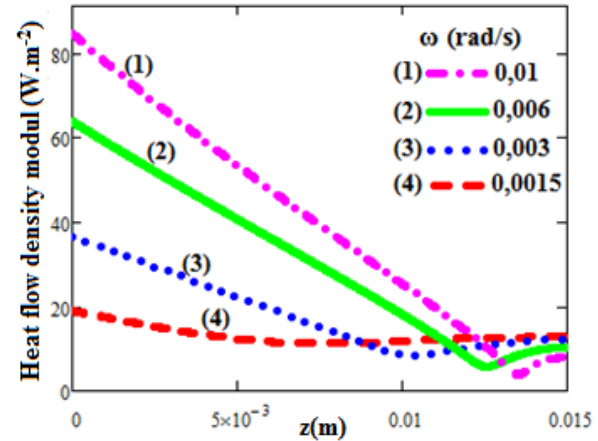


Figure 4: Evolution of heat flow density on calorimeter cover.

$r = 0.055 \text{ m}$; $h_{1z} = 25 \text{ W}/(\text{m}^2 \cdot \text{K})$; $h_{2z} = 0.05 \text{ W}/(\text{m}^2 \cdot \text{K})$.

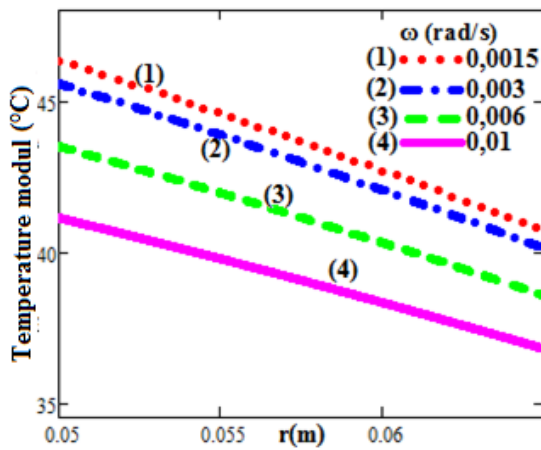


Figure 5: Evolution of temperature on lateral face of calorimeter.

$z = 0.002 \text{ m}$; $h_{1z} = 25 \text{ W}/(\text{m}^2 \cdot \text{K})$; $h_{2z} = 0.05 \text{ W}/(\text{m}^2 \cdot \text{K})$.

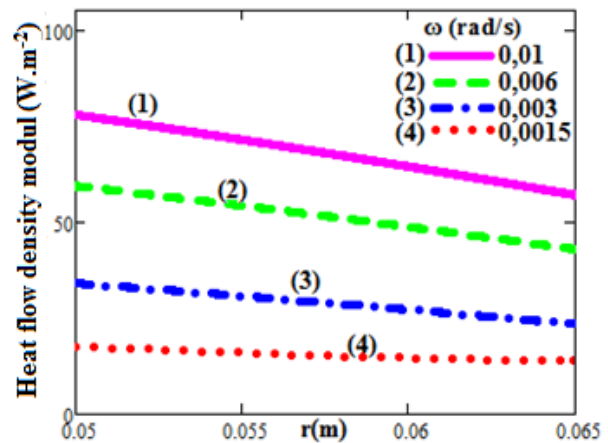


Figure 6: Evolution of heat flow density on side face of calorimeter.

$z = 0.002 \text{ m}$; $h_{1z} = 25 \text{ W}/(\text{m}^2 \cdot \text{K})$; $h_{2z} = 0.05 \text{ W}/(\text{m}^2 \cdot \text{K})$.

Evolution of temperature curves, Figures (3) and (5), shows existence of a considerable contact resistance R_C between the aluminum assumed at the temperature of solution ($T_i = 90^\circ\text{C}$) et and flax at temperature $T_F \approx 40^\circ\text{C}$.

$$T_F - T_i = R_C \cdot \phi$$

Flax material thus has a good thermal inertia to these excitatory pulsations and can be well insulation High

pulsations corresponding to relatively short periods of measurement give a better behavior of the thermal insulation.

3.2. Bode diagrams and Nyquist representations

Figures (7) and (8) respectively represent Bode diagrams of impedance and its phase for different values of depth of flax material. Figure 9 shows evolution of imaginary part of thermal impedance as a function of its real part. Phenomena are highlighted for different values of the depth of flax.

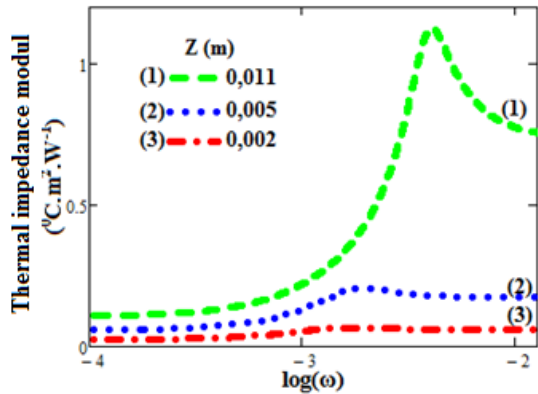


Figure 7: Variation of thermal impedance of material as a function to excitatory pulsation.

$r = 0.055 \text{ m}$; $h_{1z} = 25 \text{ W}/(\text{m}^2 \cdot ^\circ\text{C})$; $h_{2z} = 0.05 \text{ W}/(\text{m}^2 \cdot ^\circ\text{C})$

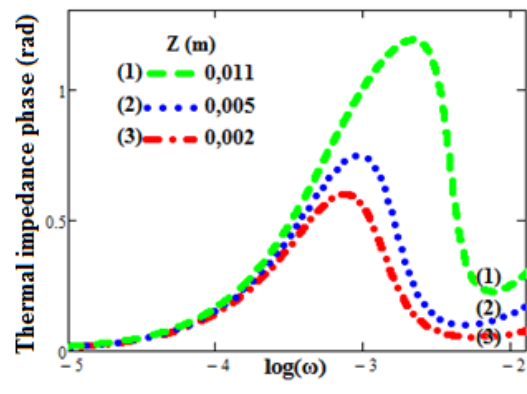


Figure 8: Variation of thermal phase as a function of exciter frequency.

$r = 0.055 \text{ m}$; $h_{1z} = 25 \text{ W}/(\text{m}^2 \cdot ^\circ\text{C})$; $h_{2z} = 0.05 \text{ W}/(\text{m}^2 \cdot ^\circ\text{C})$

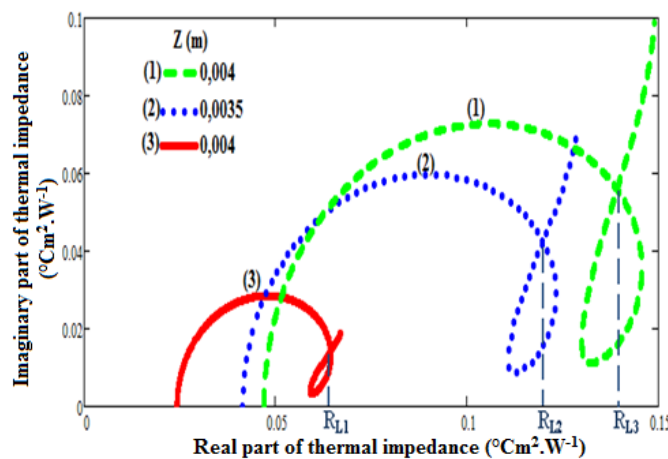


Figure 9 : Nyquist representations for different values of the depth of the material

Table 2 : Maximum values of module of thermal impedance.

Thickness z (m)	0.002	0.005	0.011
Pulsation ω (rad/s)	$1,499 \times 10^{-3}$	$1,898 \times 10^{-3}$	4.096×10^{-3}
Thermal impedance module ($^\circ\text{C} \cdot \text{m}^2 \cdot \text{W}^{-1}$)	0.06576	0.20491	1.12310

Table 3: Algebraic values of series resistance and shunt resistance

Thickness z (m)	R_s ($^\circ\text{C} \cdot \text{W}^{-1}$)	R_{sh} ($^\circ\text{C} \cdot \text{W}^{-1}$)	R_{th} ($^\circ\text{C} \cdot \text{W}^{-1}$)	R_L ($^\circ\text{C} \cdot \text{W}^{-1}$)
0.002	0.02464	0.04446	0.06874	0.06444
0.0035	0.04148	0.10270	0.14421	0.11972
0.004	0.04699	0.11314	0.16017	0.13909

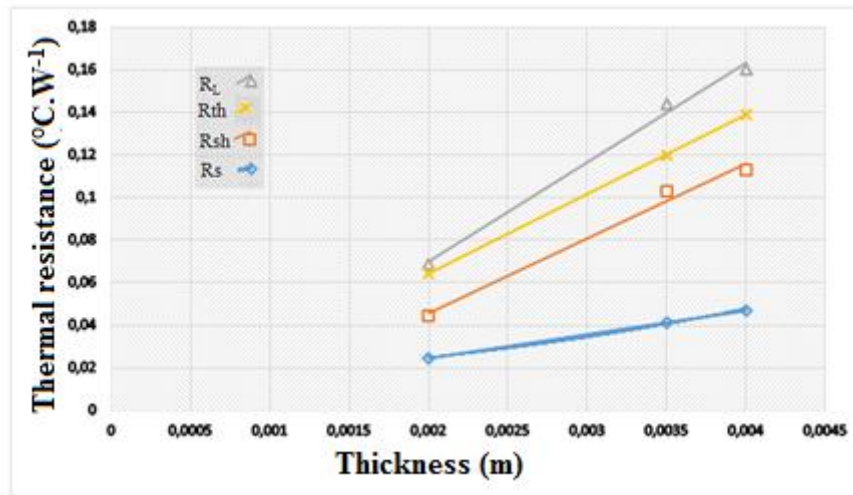


Figure 10: Evolution of resistance as function to thickness of flax material

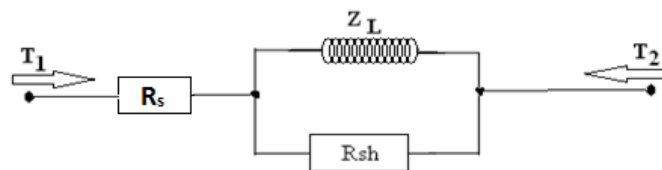


Figure 11: Equivalent electrical model of inductive phenomena of flax

For high excitation pulsations ($\omega > 10^{-3} \text{rad}\cdot\text{s}^{-1}$), thermal impedance is relatively high (Figure 7), which allows a significant retention of heat. This gives the material thermal stability. Table 2 gives some values of thermal impedance module.

Phase of impedance remains positive and has a maximum for $\omega \approx 10^{-3} \text{rad}\cdot\text{s}^{-1}$ (figure 8), This behavior is translated into electricity by inductive phenomena (Figure 11) corresponding to a return of heat to the solution in calorimeter. This phenomenon leads to an increase in calorimeter's performance.

Values of resistances given in Table 3 are obtained from the exploitation of Nquist representations (Figure 9). Figure 10 gives an evolution of resistances as a function of depth. Phenomena of thermal insulation increase linearly with the thickness of the thermal insulation.

4. Conclusion

Study shows that use of flax as a thermal insulator has considerable efficiency due to the contact resistance between aluminum and flax.

Spectroscopy of thermal impedance shows that for high excitatory pulsations we have an important module of thermal impedance.

Thermal resistance characterizes the phenomena of conduction inside the material. Quality of thermal insulator is all more important as thermal resistance is important. Thermal resistance varies linearly with thermal impedance.

References

- [1]. Mendez, F Vilaseca J. A., Pèlach M. A., Lopez J. P., Barbera L., Turon X., Gironès J., Mutje P. (2007). Evaluation of the reinforcing effect of ground wood pulp in the preparation of Polypropylene-based composites coupled with Maleic Anhydride Grafted Polypropylene; Journal of Applied Polymer Science, Vol. 105, 3588-3596.
- [2]. N. Bibi-Triki, S. Bendimerad, A. Chermiti, T Mahdjoub, B.Draoui, A. Abène. (2011). Modeling, Characterization and Analysis of the dynamic behavior of heat transfers through polyethylene and glass walls of Greenhouses. Physics Procedia 21, 67 – 74
- [3]. Makinta Boukar, Mamadou Babacar Ndiaye, Alassane Diene, Issa Diagne, Paul Demba, Fala Paye, Mohamed Sidya Ould Brahim and Grégoire Sissoko. (2014). Study of thermo-physical and mechanical



- properties of clay from the quarry of Banga Bana. *Research Journal of Applied Sciences, Engineering and Technology*. 8(20): 2126-2134..
- [4]. Y. Jannot, A. Degiovanni, G. Payet, (2009). Thermal conductivity measurement of insulating materials with a three layers device. *International Journal of Heat and Mass Transfer* 52, pp. 1105 –1111.
- [5]. M.S. Ould Brahim, I. Diagne, S. Tamba, F. Niang and G. Sissoko. (2011). Characterization of the minimum effective layer of thermal insulation material tow-plaster from the method of thermal impedance. *Research Journal of Applied Sciences, Engineering and Technology* 3(4): 337-343.
- [6]. Seydou FAYE, Mohamed Sidya OULD BRAHIM, Youssou TRAORE, Aliou DIOUF, Moussa DIENG, Abdoulaye Korka DIALLO, Issa DIAGNE, Hawa LY DIALLO, Gregoire SISSOKO. (2016). Study by Analytical Method of Transient Regime of Thermal Transfer Through a Insulation Material Tow-Plaster - Influence Coefficient of Thermal Exchange. *IPASJ International Journal of Computer Science (IIJCS)*. Volume 4, Issue 7.
- [7]. A. Diouf, I. Diagne, M.S. Oul Brahim, M.L. Sow, F. Niang and G. Sissoko. (2013). Study in cylindrical coordinates of the heat transfer through a tow material-thermal impedance. *Research Journal of Applied Sciences, Engineering and Technology* 5(22): 5159-5163.
- [8]. J.C Marechal. J.M. Devisme « Diffusivité thermique des matériaux de construction: Méthode du signal périodique ». *Anales I.T.B.T.P n° 357*, Janvier 1978.
- [9]. Y. Traore, E.B. Diaw, I. Diagne, M.B. Ndiaye, S. Tamba, B. Fleur, M. Dieng, A.K. Diallo and G. Sissoko. (2016). Characterization Phenomena of Thermal Transfer Through an Insulating Material Kapok-plaster Starting from Dynamic Impedance Method. *Research Journal of Applied Sciences, Engineering and Technology* 12(7): 712-715,
- [10]. D. Chenvidhya, K. Kirtikara, C. Jivacate, (2005). PV module dynamic impedance and its voltage and frequency dependencies. *Solar Energy Materials and Solar Cells*, Vol.86, issue 2, pp 243-251
- [11]. R. Anil Kumar, M.S. Suresh and J. Nagaraju . (2001). Measurement of AC parameters of Gallium Arsenide (GaAs/Ge) solar cell by impedance spectroscopy. *IEEE Transactions on Electron Devices*, Vol.48, No.9, Pp 2177-2179
- [12]. Cheikh Thiam, Alassane Diene, Youssou Traore, M. S. Ould Brahim, Aliou Diouf, Ould Mohamed Bah, Issa Diagne, Gregoire Sissoko. (2017), Heat Distribution in a Multilayer in Dynamic Frequency Modulation: Influence of the exciting pulse, and the thermal exchange coefficients. *Journal of Scientific and Engineering Research*, 4(9):498-505.
- [13]. Dame Diao, Alassane Diene, Mamadou Lamine Lo, Mohamed Sidya Ould Brahim1, Youssou Traore, Abdoulaye Korka Diallo, Issa Diagne, Hawa Ly Diallo, Makinta Boukar and Gregoire Sissoko. (2016). Study of thermal exchange phenomena in surface of thermal insulation kapok-plaster. *Int. J. Pure Appl. Sci. Technol.*, 33(1) - 37(2), pp. 18-25.

